



euronoise

**Acoustics'08
Paris**
June 29-July 4, 2008

www.acoustics08-paris.org

Influence of the calorimetric system setup on the output acoustic power measurement results

Antonio Petosic^a, Bojan Ivančević^a and Dragoljub Svilar^b

^aFaculty of Electrical Engineering and Computing, Unska 3, 10000 Zagreb, Croatia

^bBrodarski Institut, Avenija Većeslava Holjevcica bb, 10000 Zagreb, Croatia

antonio.petosic@fer.hr

The problem of measuring an output acoustic power using calorimetric method has been considered in the linear and nonlinear regimes of transmitter working. The transmitter with sonotrode tip has been driven at different excitation power levels and the influence of sonotrode tip position in the different calorimetric systems on the measurement results is considered. Two calorimetric systems with different volumes of loading liquid (water) and different geometries (having influence on thermodynamical losses) have been used in the experiments. The exponential experimental temperature-time curves have been fitted with theoretical and time constants, losses, output acoustic power and electroacoustic efficiency factor have been found assuming that all ultrasound energy is absorbed in the system. In the nonlinear regime of working strong cavitation activity occurs with oscillating bubbles in the front of vibrating tips and derived acoustic power is decreased because the tip is only partially radiating due to radiation impedance variations. The electroacoustic efficiency factor has been compared with equivalent circuit approach where parameters of transmitter have been found for unloaded and loaded transmitter in configurations for calorimetric method.

1 Introduction

Measurement of the acoustic power absorbed in a volume of liquid is an actual and important problem because ultrasonic surgical device can be easily characterized in that way. When vibration amplitude of the sonotrode tip is high enough, nonlinear effects in the radiating medium appear; finite amplitude effects, acoustic streaming and cavitation. These effects are very complicated to describe so derived acoustic power in the some field point is very difficult to correlate with the output source acoustic power due to nonlinear effects [1].

Measurement of the radiation pressure in the small liquid volume [2] may give mistakable results under action of multiple reflection of ultrasound waves. Usage of this methods can't give radiated or absorbed power in the liquid volume. All these drawbacks are absent if calorimetric method is used [3,4]. parameters (output power and losses) are found.

2 Calorimetric method

In calorimetric measurement setups used in the system, temperature is changed due to absorption of energy in the all parts of the system; volume of liquid, isolated PVC box and measurement equipment. The equation describing the internal energy of the system due to absorbing ultrasound waves in the liquid volume is given in the form of eq. (1).

$$\Delta U = \Delta Q = \sum_{i=1}^N m_i \cdot c_i \cdot \Delta T \quad (1)$$

ΔU [J]- total internal energy of the calorimetric system

ΔQ [J] – amount of heat energy delivered to the calorimetric system or lost by the system

m_i [kg] – mass of each individual part of calorimetric system

c_i [J/(kg °C)]– specific heat capacity of each individual part of the system

ΔT [°C]- temperature increase in the system

N - number of elements in the system

In the table 1 are shown properties of materials used in experiments, their specific heat capacities and densities. The dominant part of the system is liquid volume where the majority of ultrasound energy is absorbed.

Table 1. Properties of materials used in calorimetric experiments

Material used in calorimetry setup	Specific heat capacity c[Jkg/K]	Density of material δ [kg/m ³]
Water	4190.2	998.27
PVC plastic	880.2	880
Titanium	218.0	4507
Aluminium	336.3	2700

Multiplying masses and specific heat capacities of each individual part in the calorimetric system and adding together the total heat capacity (C_{sys}) is obtained in the form of eq. (2).

$$C_{sys} = \sum_{i=1}^N m_i \cdot c_i \quad (2)$$

Measuring the temperature increase (ΔT) in the time interval (Δt) the output acoustic power (P_a) is given with equation (3) in the form:

$$P_a = \frac{\Delta Q}{\Delta t} = \sum_{i=1}^N m_i \cdot c_i \cdot \frac{\Delta T}{\Delta t} = C_{sys} \cdot \frac{\Delta T}{\Delta t} \quad (3)$$

P_a [W]-output acoustic power

This considerations are valid when losses in calorimetric systems can be neglected so in the next sections the non-ideal (non-adiabatic and non-isothermal) calorimetric system will be considered theoretically and experimentally.

2.1 Non-isothermal and non-adiabatic calorimetric system

The non-ideal calorimeter is non-adiabatic and non-isothermal due to heat losses caused by convection, conduction and radiation. Parameters used in derivation of differential equations [3] describing temperature change in non-ideal calorimetric system are:

C_{sys} [J/°C]- the energy equivalent of calorimeter is amount of energy required to raise its temperature by 1°C under adiabatic conditions

k [J/°C]- the cooling coefficient is the amount of energy lost by a calorimeter per second for 1°C temperature difference between calorimeter and its immediate surroundings

The source power (ultrasound device or equivalent heater) P_i is in balance with energy stored in the volume of liquid (water) P_w , measurement equipment (temperature sensor) P_{app} and losses P_d which appear in the system due to heat exchange with surrounding. The losses depend on temperature difference between the liquid and the ambient temperature via the walls of the vessel and immersed equipment(4).

$$P_i = P_w + P_d + P_{app} \quad (4)$$

The energy balance can be written in the form of eq. (5).

$$C_{sys} \cdot \frac{dT_{int}}{dt} = P_i - k \cdot (T_{int} - T_o) \quad (5)$$

It is assumed that applied power $P_i(t)$ function is step function in the form of eq. (6):

$$P_i(t) = P_0 \cdot S_{[a,b]} = P_0 \cdot [H(t-a) - H(t-b)] \quad (6)$$

$S_{[a,b]}(t)$ - step function in the $[a,b]$ interval

$H(t)$ - Heaviside function

P_0 [W] -magnitude of source power $P_i(t)$

The solution in time domain is given in the form of eq. (7)

$$T_i(t) = T_0 + \frac{P_0}{k} \cdot H(t-a) \cdot \left[1 - e^{-\frac{k}{C_{sys}}(t-a)} \right] - \frac{P_0}{k} \cdot H(t-b) \cdot \left[1 - e^{-\frac{k}{C_{sys}}(t-b)} \right] \quad (7)$$

The experimental results obtained in two different calorimetric setups have been fitted with this theoretical curve. Losses and output acoustic power have been found for few different excitation levels.

2.2 Calorimetric systems setup and transmitter used in experiments

The basic calorimetric setup considered in our experiments is shown on the fig. 1. It consists of the low-frequency ultrasound device (25kHz) with internal generator, temperature sensor and foam isolated box.

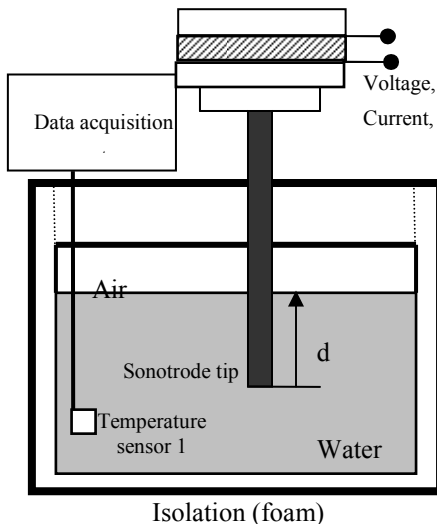


Fig. 1. Calorimetric system setup used in experiments

The immersion depth ($d=\lambda/4$ and $d=\lambda/2$) of sonotrode tip has been changed in two different configurations (Box-1 and Box 2) and output acoustic power has been compared in these different situations.

The block scheme of ultrasound transducer used in measurements with different amount of electrical power applied in the system is shown on the fig. 2.

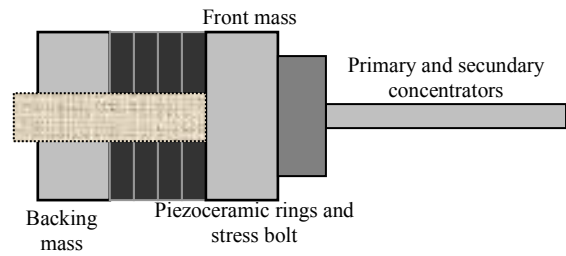


Fig. 2. Ultrasound transmitter used in measurements

The total heat capacity and heat losses in the system depend on the system geometry and the size of the isolated box. The configuration parameters with total heat capacity are shown in table 2.

Table 2. Parameters of the calorimetric system in Box 1 and Box 2

Configuration	Box 1	Box 2
M_{box} [g]	3.5	13.46
C_{box} [J/°C]	3.08	11.84
M_w [g]	49.91	99.82
C_w [J/°C]	209.13	414.075
M_{SON} [g]	0.257	0.257
C_{SON} [J/(kg°C)]	0.133	0.133
M_{TER} [g]	0.0716	0.0716
C_{TER} [J/(kg°C)]	0.024	0.024
C_{sys} [J/(°C)]	212.37	426.10

M_w [g]– mass of water in the box

C_w [J/ °C]- heat capacity of water

M_{box} [g] -PVC box mass

C_{box} [J/°C]- box total heat capacity

M_{SON} [g]- part of sonotrode mass in water

C_{SON} [J/(kg°C)]- total heat capacity of sonotrode in water

C_{TER} [J/(kg°C)]- total heat capacity of temperature sensor

C_{sys} [J/kg°C] – total heat capacity of the system

3. Experimental results-calorimetry

In this part of the work experimental results calculating output acoustic power have been shown in few measurement setups. The influence of different measurement setups (Box-1, Box-2) and the position of sonotrode tip on the output acoustic power measurements have been done. The RMS voltage and current values are written during measurements every minute together with temperature. The S[VA] applied electrical power has been calculated as product of voltage and current waveforms knowing that they are in the phase all the time during measurements. The voltage waveform is almost sinusoidal but the current isn't so the more detailed approach should be used to calculate RMS electrical power applied in the system.

2.3 Measurement results

In the linear regime of working when cavitation isn't present the measurement is difficult because there is no acoustic streaming and the temperature distribution isn't homogenous in the boxes. Here are results when applied electrical power is approximately $S_{EL}=6\text{ VA}$

Table 3. Measurement results in the Box 1 configuration and immersion depth $d=\lambda/2$

t [min]	T [°C]	U _{rms} [V]	f _{rms} [Hz]	I _{rms} [mA]	Z _{rms} [Ω]	S _{rms} [VA]
0	18,5	101,4	24709	58,19	1743	5,90
0,5	19,1	102,3	24710	59,28	1726	6,06
1	19,8	101,2	24707	59,02	1715	5,97
1,5	20,4	100,2	24708	60,3	1662	6,04
2	21,2	101,2	24708	60,2	1681	6,09
2,5	21,8	100,2	24709	59,21	1692	5,93
3	22,5	100,1	24704	59,79	1674	5,98
3,5	23,1	101,1	24700	59,69	1694	6,03
4	23,8	101,1	24699	59,62	1696	6,03
4,5	24,4	101,1	24690	59,5	1699	6,02
5	25	102,1	24690	59,24	1723	6,05
5,5	25,6	102,1	24690	59,18	1725	6,04
6	26,3	101,7	24685	59,93	1697	6,09
6,5	26,9	101,8	24685	58,3	1746	5,93
7	27,5	101,4	24690	58,45	1735	5,93

The internal temperature experimental results and their approximations with theoretical exponential curve eq. (8) are shown on fig. 3. The theoretical solution given in eq. 7 is simplified in the form of eq. 8.

$$T_e(t) = C_e - A_e \cdot e^{-\frac{(t-t_0)}{\tau}} \quad (8)$$

$T_e(t)$ – theoretical exponential curve

C_e [°C] - theoretical temperature at time $t \rightarrow \infty$

A_e [°C] - difference between temperatures at time $t=0$ min and $t \rightarrow \infty$.

τ [min] -relaxation time of thermodynamical system

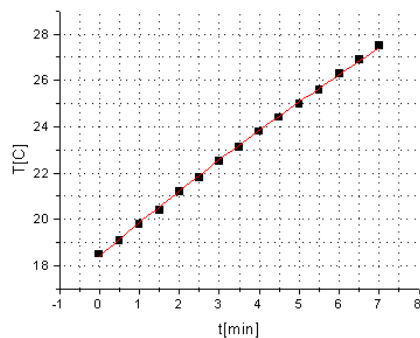


Fig 3. Approximation of experimental results with theoretical exponential curve

Parameters of exponential curve approximations (C_e, A_e, τ) with standard deviations are given in table 4. Output acoustic power and losses are calculated from approximation coefficients. Knowing losses of the calorimetric system the beginning of exponential experimental curve can be approximated with linear curve. Output acoustic power can be calculated in that way including correction due to losses in calorimetric system.

Table 4. Theoretical exponential curve approximation parameters, box1, $d=\lambda/2$

$C_e=55.96\text{ °C}$	$\Delta C_e=\pm 7.22\text{ °C}$
$A_e=37.55\text{ °C}$	$\Delta A_e=\pm 7.18\text{ °C}$
$\tau_e=25.61\text{ min}$	$\Delta \tau_e=\pm 5.63\text{ min}$
$k=0.13\text{ J}/(\text{°Cs})$	$\Delta k=0.03\text{ J}/(\text{°Cs})$
$P_{ae}=5.17\text{ W}$	$\Delta P_{ae}=1.46\text{ W}$

The beginning part of experimental curve is approximated with linear curve in the form of eq. (9) and approximation parameters (C_p, A_p) are given in table 5.

$$T_p(t) = C_p + A_p \cdot t \quad (9)$$

Linear approximation of the experimental curve shown on fig. 4.

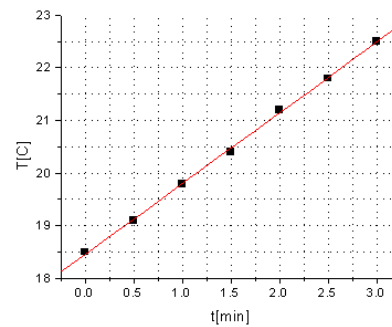


Fig. 4. Linear approximation of the beginning experimental curve [0-3min]

Parameters of linear approximations are given in table 5.

Table 5. Theoretical linear curve approximation parameters, box1, $d=\lambda/2$

$C_p=18.46\text{ °C}$	$\Delta C_p=\pm 0.03\text{ °C}$
$A_p=1.34\text{ °C}/\text{min}$	$\Delta A_p=\pm 0.018\text{ °C}/\text{min}$
$P_a'=4.73\text{ W}$	$\Delta P_a'=0.064\text{ W}$
$P_a=4.93\text{ W}$	$\Delta P_a=0.064\text{ W}$

Output acoustic power (P_a') calculated from the linear curve slope (C_p), should be corrected due to losses (k) in the calorimetric system and corrected output acoustic power (P_a) is given in the table 5. The correction factor has been calculated applying assumed exponential output acoustical power P_{ae} in the system with losses k using eq. (5). The output acoustical power P_{ae} is calculated from approximation of experimental curve with theoretical exponential. The theoretical curve for internal temperature of calorimetric system (T_i) when output acoustical power P_{ae} is applied in the system is shown on the fig.5. The heat

capacity C_{sys} and losses are assumed as in the case of the Box-1 configuration.

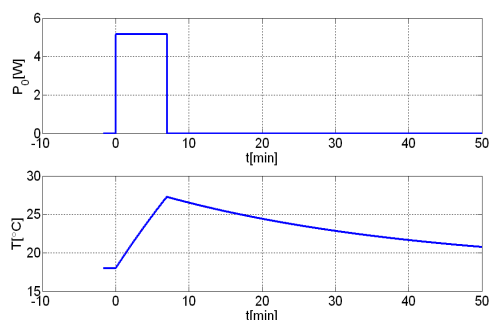


Fig. 5. Input power in the calorimetric system and corresponding theoretical internal temperature

The beginning of the theoretical curve has been approximated with linear in the first three minutes of measurement (fig. 6). The difference between applied acoustic power P_0 and calculated (three minute approximation) is used as correction factor when 3 min. approximation of experimental results is used. The correction between assumed value and calculated value in the theoretical experiment is 4.26%. The calculated value for output acoustic power P_a is 4.93 W.

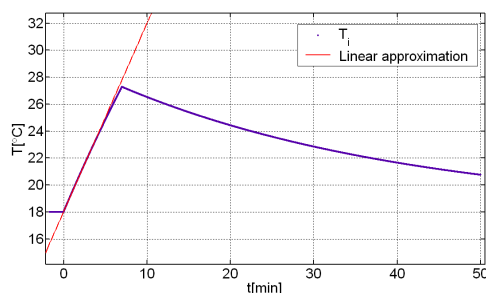


Fig. 6. Approximation of the beginning theoretical exponential curve with linear in the first three minutes

The electroacoustic efficiency factor is calculated as ratio of output acoustic and input electrical power (S[VA]) and in this case of measurement results is around $\eta_{ea}=82\%$. The procedure of measuring output acoustic power is repeated for several measurement configurations (Box-1 and 2) with different immersion depths ($\lambda/2$ and $\lambda/4$). In the table 6, results are given for the Box-1 with immersion depth $d=\lambda/4$.

Table 6. Measurement results in the box 1 configuration and immersion depth $d=\lambda/4$

t [min]	T [°C]	U_{rms} [V]	f_{rms} [Hz]	I_{rms} [mA]	Z_{rms} [Ω]	S_{rms} [VA]
0	20,7	101,2	24709	58,00	1744,83	5,87
0,5	21,6	100	24704	57,80	1730,10	5,78
1	22,2	100,3	24699	58,17	1724,26	5,83
1,5	22,8	100	24690	58,45	1710,86	5,85
2	23,4	99,9	24698	58,50	1707,69	5,84
2,5	24	100,3	24696	57,79	1735,59	5,80
3	24,5	99,1	24696	58,98	1680,23	5,84
3,5	25,1	99,9	24693	58,27	1714,43	5,82
4	25,7	100	24680	58,37	1713,21	5,84
4,5	26,2	100,9	24691	57,80	1745,67	5,83

5	26,8	100,2	24689	58,30	1718,70	5,84
5,5	27,3	99,6	24690	57,97	1718,13	5,77
6	27,9	99,9	24682	58,81	1698,69	5,88
6,5	28,4	99,2	24687	57,21	1733,96	5,68
7	28,9	100	24682	57,83	1729,21	5,78

The same procedure has been repeated as described for considered example and the results for exponential and linear curve approximations together with calculated powers are given in tables 7 and 8.

Table 7. Theoretical exponential curve approximation parameters, Box-1, $d=\lambda/4$

$C_e=52.98\text{ }^\circ\text{C}$	$\Delta C_e=\pm 4.96\text{ }^\circ\text{C}$
$A_e=32.13\text{ }^\circ\text{C}$	$\Delta A_e=\pm 4.94\text{ }^\circ\text{C}$
$t_{0e}=0\text{min}$	$\Delta t_{0e}=\pm 0\text{min}$
$\tau_e=24.36\text{min}$	$\Delta \tau_e=\pm 4.34\text{ min}$
$k=0.145\text{J}/(\text{ }^\circ\text{Cs})$	$\Delta k=0.025\text{ J}/(\text{ }^\circ\text{Cs})$
$P_{ac}=4.69\text{W}$	$\Delta P_{ac}=1.11\text{W}$

Table 8. Theoretical linear curve approximation parameters, Box-1, $d=\lambda/4$

$C_p=20.88\text{ }^\circ\text{C}$	$\Delta C_p=\pm 0.077\text{ }^\circ\text{C}$
$A_p=1.243\text{ }^\circ\text{C}/\text{min}$	$\Delta A_p=\pm 0.043\text{ }^\circ\text{C}/\text{min}$
$P_a'=4.39\text{W}$	$\Delta P_a'=0.15\text{W}$
$P_a=4.65\text{W}$	$\Delta P_a=0.15\text{W}$

The electroacoustic efficiency factor calculated in this case is $\eta_{ea}=79.9\%$. This procedure is repeated for Box-2 with different immersion depths and results for output acoustic power and electroacoustic efficiency coefficient are shown in the table 9.

Table 9. Output acoustic power measured in different calorimetric setups configurations

Configuration	P_{ac} [W]	k [J/($^\circ\text{Cs}$)]	P_a [W]	η_{ca} [%]
Box-2, $d=\lambda/2$	5.16	0.16	4.72	79.19
Box-2, $d=\lambda/4$	5.016	0.16	4.56	78.35
Box-1, $d=\lambda/2$	5.17	0.13	4.93	82
Box-1, $d=\lambda/4$	4.69	0.12	4.65	79.9

It can be seen that in strong cavitation regime of working there is no influence on output acoustic power results.

3 Experimental results of transmitter electromechanical characterization

The input electrical impedance has been measured in the frequency range near series resonance frequency of transmitter when sonotrode tip is in the complex geometry, where radiation impedance depends on the complex pressure field in the system. The input electrical impedance is measured when transmitter is unloaded in air, loaded in the free field conditions and loaded in the complex geometry configurations for calorimetric measurements.

The real part of input admittance in air and in water in free field with immersion depth $d=\lambda/4$ is shown on the figure 7.

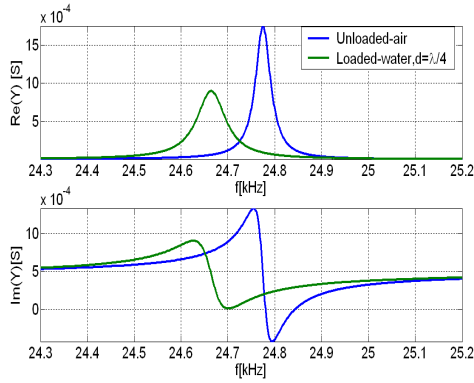


Fig. 7. Comparison of measured input electrical admittances (loaded and unloaded transmitter)

It can be seen that resonance frequency is decreased in water due to oscillating mass of water which is included in motion with transmitter tip. The results of measured input electrical impedance parameters are given in the table 11.

Table 11. Measured electrical parameters of transmitter radiating in air and in the water

	R_0 [MΩ]	C_0 [nF]	f_s [Hz]	f_p [Hz]	Q_m	R_i [Ω]
Air	57	2.79	24775	24848	619.4	570.43
Water $d=\lambda/4$	19	2.79	24665	24737	333.3	1110
Box-1 $d=\lambda/4$	19	2.79	24653	24726	410.8	835.43
Box-1 $d=\lambda/2$	29.3	2.71	24662	24733	493.2	722.76
Box-2 $d=\lambda/4$	19	2.79	24656	24731	440.3	904.96
Box-2 $d=\lambda/2$	26.8	2.8	24666	24739	373.7	1224.1

The significance difference in the real part of radiation impedance causes that the electroacoustic efficiency factor (η) is different when sonotrode tip is located in different points of complex pressure fields in the calorimetric geometry. The results for equivalent circuit parameters and electroacoustic efficiency coefficients are given in the table 12.

Table 12. Measured parameters of transmitter radiating in air and in the water

	L_1 [H]	C_1 [pF]	R_{rad} [Ω]	Q_t	η [%]
Air	2.50	0.16	0	651.9	-
Water $d=\lambda/4$	2.55	0.16	539.57	352.4	46.19
Box-1 $d=\lambda/4$	2.51	0.165	265	456.3	33.62
Box-1 $d=\lambda/2$	2.66	0.156	152.33	560.5	20.35
Box-2 $d=\lambda/4$	2.45	0.169	334.53	410.9	28.88
Box-2 $d=\lambda/2$	2.51	0.165	653.76	410.9	39.64

The electroacoustic efficiency factor is calculated assuming that part of applied electrical power is lost in mechanical

and dielectrical losses. Only part of the applied power is radiated in loading medium.

4 Conclusion

In this work the output acoustic power of ultrasound transducer has been measured by calorimetric method using different geometrical configurations of calorimetric setup. The immersion depth and size of boxes doesn't have significant influence on the obtained calorimetric results at higher excitation levels when strong cavitation is present. The influence on output acoustic power is significant when cavitation isn't so strong. In that regime of working the position of sonotrode tip determinates the output acoustic power and electroacoustic efficiency factor.

The input electrical impedance of transducer at low excitation signal (1V) has been measured in different calorimetry setups and the electroacoustical efficiency factor (η) has been compared with one obtained using calorimetry method (η_{ca}) in the strong nonlinear regime of working. The results show significant spatial dependency of real part of radiation impedance in calorimetric boxes. There is significant difference between results obtained using calorimetric method and electromechanical characterization.

References

- [1] IEC 6147: Ultrasonic surgical systems, Measurements and declaration of the basic output characteristic, 1998-1A
- [2] IEC61088: Characteristics and measurements of ultrasonic piezoceramic transducers, 1991
- [3] M.A.Margulis, I.M.Margulis: Calorimetric method for measurement of acoustic power absorbed in a volume of liquid, Ultrasonic Sonochemistry 10, 2003, 343-345
- [4] J.K. Zieniuk, B. Evans: The influence of thermal parameters on making ultrasound power measurements by a calorimetric method, Acustica, Vol 25. (1971)